Atmos. Meas. Tech. Discuss., 3, 1615–1644, 2010
www.atmos-meas-tech-discuss.net/3/1615/2010/

Atmospheric Measurement Techniques Discussions

This discussion paper is/has been under review for the journal Atmospheric Measurement Techniques (AMT). Please refer to the corresponding final paper in AMT if available.

Remotely operable compact instruments for measuring atmospheric CO_2 and CH_4 column densities at surface monitoring sites

N. Kobayashi[1], G. Inoue[1], M. Kawasaki[2], H. Yoshioka[2], M. Minomura[2], I. Murata[3], T. Nagahama[4], Y. Matsumi[4], and T. Ibuki[2]

[1]Research Institute for Humanity and Nature, Kyoto 603-8047, Japan
[2]Department of Molecular Engineering, Kyoto University, Kyoto 615-8510, Japan
[3]Department of Geophysics, Tohoku University, Sendai 980-8578, Japan
[4]Solar Terrestrial Environment Laboratory, Nagoya University, Nagoya 464-8601, Japan

Received: 8 March 2010 – Accepted: 19 March 2010 – Published: 12 April 2010

Correspondence to: M. Kawasaki (kawasaki@moleng.kyoto-u.ac.jp)

Published by Copernicus Publications on behalf of the European Geosciences Union.

Abstract

Remotely operable compact instruments for measuring atmospheric CO_2 and CH_4 column densities were developed in two independent systems: one utilizing a grating-based desktop optical spectrum analyzer (OSA) with a resolution enough to resolve rotational lines of CO_2 and CH_4 in the region of 1565–1585 and 1674–1682 nm, respectively; the other is an application of an optical fiber Fabry-Perot interferometer (FFPI) to the CO_2 column density. Direct sunlight was collimated via a small telescope installed on a portable sun tracker and then transmitted through an optical fiber into the OSA or the FFPI for optical analysis. The near infrared spectra of the OSA were retrieved by a least squares spectral fitting algorithm. The CO_2 and CH_4 column densities deduced were in excellent agreement with those measured by a Fourier transform spectrometer with high resolution. The rovibronic lines in the wavelength region of 1570–1575 nm were analyzed by the FFPI. The I_0 and I values in the Beer-Lambert law equation to obtain CO_2 column density were deduced by modulating temperature of the FFPI, which offered column CO_2 with the statistical error less than 0.2% for six hours measurement.

1 Introduction

Carbon dioxide and methane are the most important anthropogenic greenhouse gases, with a contribution of 80% of radiative forcing due to greenhouse gasses, leading to global warming (IPCC 2001). In order to determine major source and sink regions on the earth, precise measurement of the global column density is an extremely pressing need. A greenhouse gas observing satellite (GOSAT: IBUKI) of Japan was launched on 23 January 2009. Data acquisition for the CO_2 and CH_4 column densities has progressed by an onboard Fourier transform spectrometer, FTS (Kuze et al., 2009). GOSAT observes an instantaneous field of view 10.5 km in diameter at every 160 km interval (Kuze et al., 2009; Yokota et al., 2009). For validation of the GOSAT data and also for covering the regions between the sparsely meshed observing points of GOSAT,

AMTD

3, 1615–1644, 2010

it has been necessary to develop an apparatus with a high accuracy for measurement of the column density at surface monitoring sites. FTS with high resolution analyzing direct sunlight offers enough sensitivity (Washenfelder et al., 2006; Oyama et al., 2009) for this, and thus 11 ground-based FTIR spectrometers have been operated for the network of SCIAMACHY (Dils et al., 2006). FTS instruments, however, have a high cost and are unsuitable for portable use.

In the present paper a desktop optical spectrum analyzer (OSA: Yokogawa Electric, AQ6370B-Custom) monitoring the near infrared (NIR) region was examined for applicability to measure CO_2 and CH_4 column densities in air. Spectral resolution of the OSA is higher than that of the FTS onboard GOSAT. Rotational lines in the regions of 1565–1585 and 1665–1685 nm were resolved for CO_2 and CH_4 measurements, respectively. The OSA instrument employed here is compact, portable, easy to use, rugged and inexpensive.

As for the other method to measure atmospheric CO_2 column density, Wilson et al. (2007) have reported that a Fabry-Perot interferometer made of quartz glass has a high enough spectral resolution for resolving the rotational photoabsorption lines centered at 1575 nm (Wilson et al., 2007). A prototype instrument presented by them was composed of a solid etalon Fabry-Perot interferometer, off-axis parabolic mirrors, a beam splitter etc. The instrument is compact but seems to need precise optical alignment. In addition, the solid etalon has an appreciable heat capacity and hence temperature control of the solid etalon would be difficult within 1/100 deg accuracy for keeping the transmission wavelength through the etalon fixed (Wilson et al., 2007). Fiber Fabry-Perot interferometer (FFPI), which has been developed for use in telecommunication industry, has the same optical features with the solid Fabry-Perot interferometer, and thus was tried to measure the CO_2 column density in the present work. The FFPI instrument assembled by simple fiber optics is essentially optical alignment-free, compact, easy to set up and strong against shock. Since the FFPI has a small heat capacity, transmission wavelength of the FFPI quickly responds to temperature change to reduce the time interval for measurement of the CO_2 column density.

AMTD
3, 1615–1644, 2010

2 Instrumental designs

2.1 Collimation of sunlight

A small telescope was designed to collimate sunlight onto an optical fiber: The sunlight was prefiltered by a long-pass filter (HOYA R100, $\lambda \geq 1000$ nm) and then focused by a lens (50 mm in diameter and $f = 100$ mm) on an optical fiber. The sunlight through the optical fiber was transmitted into the OSA or FFPI analyzer. The small telescope was onboard a portable sun tracker with a GPS (Prede, ASTX-2, 25 kg).

2.2 Optical spectrum analyzer (OSA)

An optical spectrum analyzer made by Yokogawa AQ3670B-Custom disperses radiation in the wavelength regions of 600–1800 nm and is sensitive down to −90 dBm or 1 pW. The incidence slit width is designed to be equal to a core-diameter of an optical fiber. A multimode optical fiber (MMF) with 62.5 µm in core-diameter was found to transform a practically analyzable photon flux and to give an FWHM = 0.16±0.01 cm^{-1} at 1572 nm measured by using a tunable laser (ANDO, AQ4321D).

Typical photoabsorption lines of the atmospheric CO_2 measured by the OSA are shown in Fig. 1, which was scanned in a 34 s period. The intensity of the sunlight in the scanning interval sustained fluctuation of air or shielding by thin cloud. For compensating the fluctuation of the sunlight intensity, 1000–1700 nm radiation was monitored throughout the measurement (gray line in Fig. 1a). Optical bundle fibers were adopted for the monitoring the sunlight intensity. Photons through the central optical fiber were supplied for the spectral analysis and those outer fibers were recorded to be reference signal and utilized for normalization of the raw spectrum.

2.3 Fiber Fabry-Perot interferometer (FFPI)

The instrument described here employs a single mode optical fiber (SMF) FFPI to measure the CO_2 column density through photoabsorption of sunlight. In this design, the

AMTD
3, 1615–1644, 2010

sunlight passes through the atmosphere where it undergoes some photoabsorption by atmospheric CO_2. The NIR radiation of 1570–1575 nm where strong CO_2 photoabsorption lines lie was isolated via a narrow bandpass filter, which was made of a quartz glass (Optical Coatings Japan) and installed at the incidence of the optical fiber. The isolated radiation was fed into a 2×2 optical coupler of SMF (Tatsuta Electric Wire & Cable) to split into two channels with transmitting intensity ratio of 10:1 where the first stronger channel is for the spectral analysis by the FFPI (Nippon Electric Glass, 13 mm long × 1.25 mm in diameter) (Sakamoto and Nishii, 2005) and the second weaker one is for reference signal. Output intensity of the FFPI reached several nW and was sufficient for measurements. The FFPI and the optical coupler were set in a small incubator kept at 25 °C.

The FFPI was directly jacketed with a low-expansion glass ceramic shroud, and gave a free spectral range (FSR) shown in Fig. 2. The FFPI transmittance fringes were aligned with spacing of the CO_2 photoabsorption lines (Devi et al., 2007) so that photoabsorption due to CO_2 is primarily detected and gives the I_0 and I values in the Beer-Lambert law as will be discussed below. The sunlight intensity via the second channel strongly depended on changes of the NIR solar flux and was recorded as reference signal with 200 ms interval. This fast time response was required to follow the rapid solar flux intensity change that is probably caused by temporal air-fluctuation and shielding by clouds. The signal ratios of the two channels were used to infer the atmospheric CO_2 abundance.

The FFPI has a temperature coefficient toward the transmittance wavelength as shown in Fig. 2b and thus the solar light wavelength passing through the FFPI is able to be on- and off-aligned with CO_2 photoabsorption lines by controlling the temperature with a Peltier device (Cell System, TDU-5000R, <150 VA). When the NIR radiation passed through the FFPI most matches the spacing of the CO_2 rotational lines, the detector gives the minimum intensity which effectively corresponds to the I value in the Beer-Lambert law. At the minimum spectral matching the maximum intensity is

recorded which corresponds to the I_0 value:

$$\ln(I_0/I) = \sigma_t \times N \times L \quad (1)$$

where σ_t is the effective total photoabsorption cross section of CO_2 in the measuring wavelength region of this instrument, N the concentration of CO_2 in a unit volume, and L the length from the earth's surface to the space. The product $N \times L$ is the CO_2 column density and determinable when the σ_t is available for the optical system employed. A laptop computer for controlling the temperature of the FFPI works as a data acquisition part, recording spectra as well as geophysical and meteorological data from the GPS unit installed in the sun tracker.

3 Performance tests

3.1 Optical spectrum analyzer (OSA)

Figure 3 shows parts of photoabsorption spectra of CO_2 observed by the OSA (solid curve) and the FTS onboard GOSAT (gray line with dots). The optical resolution of the former is better than that of the latter.

One of the campaigns for the validation of the GOSAT measurements was carried out as a joint program of the Japan Aerospace Exploration Agency (JAXA) and the National Institute for Environmental Studies of Japan (NIES) on 26 August 2009 at the Moshiri observatory of Nagoya University in Hokkaido Japan (Latitude 44.366; Longitude 142.26; 290 m a.s.l.). The following instruments and an aircraft participated in the campaign: a ground-based Bruker 120HR FTS, an aircraft to collect flask samples for CO_2 and CH_4 in the air, balloons to measure pressure, temperature, relative humidity and atmospheric CO_2 concentration over the Moshiri observatory, and an OSA (Yokogawa AQ6370B-Custom). Direct sunlight was dispersed by the FTS and the OSA under the same weather conditions. The spectra of the FTS and the OSA were retrieved by adopting a nonlinear least squares spectral fitting algorism developed for

the present work, details of which are given in the Appendix. The FTS spectra were independently retrieved by NIES using GFIT.

3.1.1 CO_2 column density

Spectra shown in Fig. 1 were observed by the OSA and the FTS dispersing sunlight on 26 August 2009 at Moshiri observatory of Nagoya University in Hokkaido Japan, where the spectral resolution of the Bruker 120HR FTS was set at 0.02 cm^{-1}. Figure 4 shows enlarged views of the spectra after the retrievals using the peak fitting algorism given in the Appendix. The atmospheric CO_2 column densities obtained by the OSA and the FTS measurements are given in Table 1 for dry air. Relative humidity, temperature and pressure in the air were measured over the Moshiri observatory up to 26 km and took account of in calculating the column densities.

A balloon with a well-calibrated CO_2 sensor was launched at 13:30 in order to directly measure CO_2 profile over the Moshiri observatory and the CO_2 concentrations were accumulated till 14:26 (T. Nakayama and S. Takekawa, personal communication, 2009). The CO_2 concentration measured was 374.4±3.6 ppm on the surface level and 388.8±2.3 ppm at 10 km. The column density deduced from the concentrations is given in Table 1 where the atmospheric CO_2 concentration above 10 km was treated after the method in evaluation of CO_2 column average volume mixing ratio (VMR) over Tsukuba (Araki et al., 2010). The CO_2 concentration in the stratosphere above 20 km is considered to be five years older than that of the global mean concentration of CO_2 in the troposphere, which is 385.2 ppm in 2008 with a growth rate of 1.93 ppm/yr (WMO, 2008). Thus the CO_2 concentrations in the troposphere and the stratosphere in 2009 are estimated to be 387.1 and 377.6 ppm, respectively. Between 10 km and 20 km in altitude the concentration is assumed to be linear (Araki et al., 2010).

The OSA, the FTS and the balloon measurements give the CO_2 column density of $(7.875\pm0.055)\times10^{21}$ molecules/cm^2, being in excellent agreement. The present observation strongly implies that the OSA has the performance enough to measure the CO_2 column density as well as FTS used for a ground-based standard.

AMTD
3, 1615–1644, 2010

Atmospheric CO_2 column densities measured by GOSAT have been officially announced and are quoted in Table 1 for 6 August and 2 September 2009. The column densities of GOSAT were measured over Nayoro City in Hokkaido Japan located 20 km east to the Moshiri observatory. The values of GOSAT for the days are in consistent with those of the OSA, the FTS and the balloon.

Figure 5 shows profiles of the CO_2 column densities measured by the four independent instruments in Table 1. A little large distribution of the column densities in the FTS (small open circles) probably arises from thin clouds since it was cloudy in the morning at the Moshiri distinct on 26 August 2009. The weather improved in the afternoon but was not cloud-free. The column density of CO_2 measured at the Tall Tower site in Wisconsin USA has shown similar distribution of the CO_2 columns on a partly cloudy day (Washenfelder et al., 2006). Reference signal correction for the OSA spectra (large open circles) seems to be effective for a better distribution.

In the present retrievals the CO_2 concentration in the air is a fitting parameter and assumed to be constant (see Appendix A). The values thus deduced correspond to the column average VMR of CO_2 in dry air, which is defined as the ratio of the deduced column density of CO_2 to total column of dry air (Washenfelder et al., 2006):

$$\text{Column average VMR of } CO_2 = [\text{column of } CO_2]/[\text{total column of dry air}] \quad (2)$$

The column average VMR for the balloon measurement is calculated to be 378.02±5.16 ppm and lies in consistent with those of the OSA and the FTS. The total column of dry air in Eq. (2) is replaced by the following relation (Washenfelder et al., 2006):

$$[\text{total column of dry air}] = [\text{column of } O_2]/0.2095 \quad (3)$$

where the dry-air mole fraction of O_2 is 0.2095 and highly constant in the air. The Eq. (2) abbreviated to xCO_2 is then given by

$$xCO_2 = 0.2095 \times [\text{column of } CO_2]/[\text{column of } O_2] \quad (4)$$

The FTS spectra from 09:50 to 16:01 were retrieved by NIES using GFIT (denoted by FTS-GFIT hereafter) and the xCO_2 values were deduced by Eq. (4). The arithmetic mean of the xCO_2 for 275 retrievals in the FTS-GFIT was 377.05±2.47 ppm as given in Table 1. Flask samples of the atmospheric CO_2 were collected by the aircraft from 530 to 7300 m over the Moshiri observatory and the CO_2 concentration was analyzed by NIES. We obtain the column average VMR or xCO_2 to be 376.56±0.02 ppm for the flask sampling if we assume that the CO_2 concentration of 375.85±0.01 ppm at 7300 m continues up to 10 km. Above 10 km the same assumption in the balloon discussion was applied. The xCO_2 values by the aircraft and the FTS-GFIT are in excellent agreement with those for the OSA, the FTS and the balloon in Table 1. However, the xCO_2 for GOSAT is clearly low. It has been announced that the xCO_2 of GOSAT lies lower than expectation of an offline global atmospheric transport model developed by NIES (NIES TM) by 10–15 ppm (Yokota et al., 2009). The reason to give the low xCO_2 is now under review.

Figure 6 shows the xCO_2 profiles of the OSA (large open circles) and the FTS (small open circles) retrievals by use of the present fitting algorism as well as the FTS-GFIT (small solid circles). Most of the data concentrate at 377 ppm but some points of the FTS distribute a little wide probably due to shielding effect by thin cloud. The xCO_2 distribution of the OSA is good because of the reference signal correction.

3.1.2 CH_4 Column density

Photoabsorption spectrum of CH_4 measured by Yokogawa AQ6370B-Custom on 26 August 2009 at the Moshiri observatory was retrieved for an estimation of the CH_4 column density. Two peaks at 1674.447 and 1677.601 nm in Fig. 7 were used for the retrieval. The column densities and column average VMRs deduced are shown in Fig. 8. The column densities and the xCH_4 values are stable all day long, which are numerically given in Table 2 along with the GOSAT observation. Agreements between them are excellent.

AMTD
3, 1615–1644, 2010

The xCH$_4$, being a fitting parameter in the present retrieval, is given in Table 2 as well as the FTS-GFIT retrieval, the aircraft and GOSAT. The xCH$_4$ for the aircraft was calculated by use of the estimation for the balloon measurement. That is, the concentration of 1.850 ppm sampled at 7300 m was assumed to continue up to 10 km. The global mean concentration of CH$_4$ in 2008 is 1.797 ppm with a growth rate of 2.5 ppb (WMO, 2008), giving 1.787 ppm for the stratospheric concentration above 20 km in 2009. The CH$_4$ concentration between 10 and 20 km linearly decreases from 1.850 to 1.787 ppm. We think that the AQ6370B-Custom OSA is usable to elucidate the CH$_4$ column average VMR in the air.

From the analyses above mentioned we conclude that the compact OSA is a powerful tool to measure the CO$_2$and CH$_4$ photoabsorption spectra in the air and the column densities are retrieved as well as FTS. A portable and remotely operable OSA measures the CO$_2$ and CH$_4$ column abundances at any place where electric power is available and will cover the area between the large-meshed observing points of GOSAT.

3.2 Fiber Fabry-Perrot interferometer (FFPI)

A spectral profile of the sunlight passing through the narrow bandpass filter is shown in Fig. 9, where the sharp dips superimposed on the peak are assigned to the R-branch lines in the 30 012←00 001 band of CO$_2$ (Devi et al., 2007). The spacing of the CO$_2$ photoabsorption lines between R8e and R22e is 0.324±0.016 nm, which is close to the FRS=0.317±0.002 nm of the FFPI in Fig. 1. The peak width of the transmitted radiation through the FFPI is $\Delta\lambda$=0.072±0.002 nm at FWHM, which is wider than the pressure broadening of the R00e line of CO$_2$, i.e. 0.050 nm at 1013 hPa (Nakamichi et al., 2006). The temperature coefficient of the FFPI was found to be 13.58±0.16 pm/deg by monitoring wavelength shift of the transmitted light in Fig. 2.

By modulating the temperature of the FFPI between 30 and 45 °C (dotted curve in Fig. 10), the wavelength transmitted through the FFPI shifted and hence the signal intensity via the FFPI periodically changed as shown by the solid curve in Fig. 10. In a cycle of the temperature modulation, the highest value gives the I_0 while the lowest

one corresponds to the l in Eq. (1). Small dip in the peak-top results from overshooting the temperature to give a minimum overlap between the FSR and the spacing of CO_2 photoabsorption lines. The hump in the bottom, which is opposite, results from overshooting the temperature to give a maximum overlap. The dip and hump ensure the maximum and the minimum signal intensities, respectively.

To obtain the effective total photoabsorption cross section, σ_t, a calibration curve in Fig. 11 was measured by changing CO_2 pressure in a photoabsorption cell (l=174.1 cm) in the laboratory. The slope gives the effective total photoabsorption cross section $\sigma_t=(2.696\pm0.051)\times10^{-23}$ cm^2/molecule, which is larger than that for the strongest line of R16e with an intensity of 1.7414×10^{-23} cm^2/molecule (Devi et al., 2007) because some rotational lines contribute to the effective σ_t. By adopting the σ_t cross section, the CO_2 slant column is calculated by Eq. (1). Airmass correction approximated by the following formula should be performed in obtaining the CO_2 column density (Kasten and Young, 1989):

$$\text{Airmass} = 1/[\cos(Z) + 0.50572 \times (96.07995 - Z)^{-1.6364}] \quad (5)$$

where Z is the solar zenith angle.

The CO_2 column density thus obtained, however, is only apparent since the effective total photoabsorption cross section σ_t was determined under artificial conditions in the laboratory. For accessing a true value the temporal column density should be normalized by CO_2 column density measured by a standardized instrument. We measured the atmospheric CO_2 column densities by use of the FFPI and the OSA under the same weather conditions at the Katsura campus of Kyoto University in Kyoto Japan (Longitude 34.983, Latitude 135.677, 160 m a.s.l.). An example of the normalized FFPI measurements is shown in Fig. 12. The OSA measurements shown by the solid circles give the column density of $(7.93\pm0.06)\times10^{21}$ molecules/cm^2 and the that revised by normalizing parameter for the FFPI shown by the open circles is $(7.94\pm0.01)\times10^{21}$ molecules/cm^2 on 31 October 2009. It is clear that statistics of the distribution for the FFPI is much better than that for the OSA. Standardizing parameter

in the revising procedure of the FFPI should be determined one time for the individual FFPI instrument because the effective σ_t cross section depends strongly on the bandwidth and the transmission efficiency of the sunlight through the narrow pass filter employed.

The instrument composed of an FFPI optical device for obtaining the CO_2 column density is much less expensive and easier to operate than the OSA, though it needs to be calibrated and normalized one time by means of a standardized instrument. The fiber devices employed in the present work are essentially optical alignment-free, therefore rugged, and will perform their function at surface sites which may be unsuitable for FTS or OSA instruments.

4 Concluding remarks

Two instruments presented here demonstrate the capability of compact, easy-to-operate, portable, and remotely operable measurement of the atmospheric column density: An optical spectrum analyzer (OSA) with high enough resolution to resolve rotational lines of CO_2 and CH_4, in comparison with a Fourier transform spectrometer (FTS) onboard GOSAT. Using a least squares spectral fitting algorithm developed for the present work, the OSA gives atmospheric CO_2 and CH_4 column densities which beautifully agree with those obtained by a ground-based FTS with high resolution of $0.02\,cm^{-1}$ and a balloon measurement, and are in agreement with the GOSAT records. The column average concentrations of CO_2 and CH_4 were deduced as a parameter in the present retrievals and they are in excellent agreement with those determined by flask samples by an aircraft, the FTS spectra retrieved by GFIT and the balloon. The xCO_2 of GOSAT is a little low (Yokota et al., 2009).

A fiber etalon Fabry-Perot interferometer (FFPI), modelled after the work of Wilson et al. who used a solid Fabry-Perot interferometer (Wilson et al., 2007), is modified for measuring the atmospheric CO_2 column density by adopting optical fiber devices. The optically simple, inexpensive and light weighted FFPI instrument has high precision

(statistical error <0.2%) and fast temperature response though it needs normalization one time by means of a standardized instrument such as OSA or FTS. Measured data are made available on the World Wide Web.

Appendix A

Data analysis

Photoabsorption spectra of the atmospheric CO_2 and CH_4 measured by the OSA and the FTS were analyzed with a line-by-line algorithm which was originally developed by I. M. and revised by N. K. and H. Y. for the present CO_2 and CH_4 column densities. Principal concept of the analysis is similar to that of a profile retrieval algorithm of GFIT or SFIT2 widely used in FTIR community. The present fitting program is corded so that data in ASCII format are directly analyzable since the OSA produces data file with csv extension. Photoabsorption line shape was approximated by means of the Voigt function, whose rapid computation has been reported by Drayson (Drayson, 1976). Original data recorded by the Bruker 120HR FTS were converted into ASCII data sheet with dpt extension by use of an OPUS program.

In the forward model calculations the atmosphere up to 48 km was divided into 28 vertical layers. The slant column density was derived by a least squares fit of the forward model for the spectra in the regions of 1570–1574 and 1673.8–1677.7 nm for CO_2 and CH_4, respectively. Photoabsorption due to H_2O was checked by the HITRAN 2008 database and took account of in the retrievals.

The nonlinear least squares spectral fitting algorithm requires several input parameters. They are SZA, the spectral line parameters for the photoabsorption, a priori profiles of VMR for CO_2, CH_4 and H_2O, atmospheric temperature, pressure, relative humidity, solar spectrum and instrumental line shape (ILS). Geographical information including the SZA for each run, longitude, latitude and above sea level was directly obtained via the GPS in the sun tracker. The profiles of temperature, pressure, and

relative humidity above 500 m were obtained from a radiosonde observation measured on 26 August 2009 over the Moshiri observatory. The meteorological data on the surface were monitored by a pressure transducer (Setra, 276) and 2 sensors for temperature and relative humidity (Sensirion, SHT71) during the run. A fitting parameter corresponding to the column average concentration of CO_2 or CH_4 in the air was assumed to be constant. The ILS for the AQ6370B-Custom OSA was approximated by a triangle. Full width at half maximum (FWHM) of the triangle was the second parameter to get the best fitted spectrum and found to be 0.168 cm^{-1} for the incidence of a MMF with 62.5 µm in core-diameter employed. The ILS for the Bruker 120HR FTS was a boxcar with a width of 0.02 cm^{-1}.

Acknowledgements. The authors express sincere thanks to T. Yokota and I. Morino of NIES for offering us the solar spectrum, the retrieval results by GFIT and the flask sampling data by aircraft, and T. Nakayama and S. Takekawa of Nagoya University for providing the concentrations of CO_2 measured by balloon before publication. We also thank NIES and the Japan Weather Association (JWA) for providing the meteorological data measured over the Moshiri observatory, Yokogawa Electric Co. Ltd. for renting the optical spectrum analyzer gratis, Nippon Electric Glass Co. Ltd. for providing the fiber etalon Fabry-Perot interferometer optical devices, and Nishimura Co. Ltd. for designing the collimation system of the near infrared radiation of the sun.

References

Araki, M., Morino, I., Machida, T., Sawa, Y., Matsueda, H., Yokota, T., and Uchino, O.: CO_2 column-averaged volume mixing ratio derived over Tsukuba from measurements by commercial airlines, Atmos. Chem. Phys. Discuss., 10, 3401–3421, 2010, http://www.atmos-chem-phys-discuss.net/10/3401/2010/.

Devi, V. M., Benner, D. C., Brown, L. R., Miller, C. E., and Toth, R. A.: Line mixing and speed dependence in CO_2 at 6348 cm^{-1}: Positions, intensities, and air- and self-broadening derived with constrained multispectrum analysis, J. Molec. Spectrosc., 242, 90–117, 2007.

Dils, B., De Mazière, M., Müller, J. F., Blumenstock, T., Buchwitz, M., de Beek, R., Demoulin, P., Duchatelet, P., Fast, H., Frankenberg, C., Gloudemans, A., Griffith, D., Jones, N., Kerzenmacher, T., Kramer, I., Mahieu, E., Mellqvist, J., Mittermeier, R. L., Notholt, J., Rinsland, C. P., Schrijver, H., Smale, D., Strandberg, A., Straume, A. G., Stremme, W., Strong, K., Sussmann, R., Taylor, J., van den Broek, M., Velazco, V., Wagner, T., Warneke, T., Wiacek, A., and Wood, S.: Comparisons between SCIAMACHY and ground-based FTIR data for total columns of CO, CH_4, CO_2 and N_2O, Atmos. Chem. Phys., 6, 1953–1976, 2006, http://www.atmos-chem-phys.net/6/1953/2006/.

Drayson, S. R.: Rapid computation of the Voigt profile, J. Quant. Spectrosc. Ra., 16, 611–614, 1976.

IPCC: Climate change 2001: The Scientific Basis, Contribution of Working Group I to the Third Assessment Report of the Intergovernmental Panel on Climate Chang, edited by: Houghson, J. T., Ding, Y., Criggs, D. J., Noguer, N., van der Linden, P. J., Dai, X., Maskell, K., and Johnson, C. A., Cambridge University Press., United Kingdom and New York, NY, USA, p. 6., 2001.

Kasten, F. and Young, A. T.: Revised optical air mass tables and approximation formula, Appl. Optics, 28, 4735–4738, 1989.

Kuze, A., Suto, H., Nakajima, M., and Hamazaki, T.: Thermal and infrared sensor for carbon observation Fourier-transform spectrometer on the Greenhouse Gases Observing Satellite for greenhouse gases monitoring, Appl. Optic. 48, 6716–6733, 2009.

Nakamichi, S., Kawaguchi, Y., Fukuda, H., Enami, S., Hashimoto, S., Kawasaki, M., Umekawa, T., Morino, I., Suto, H., and Inoue, G.: Buffer-gas broadening for the (3 0^0 1) III←(0 0 0) band of CO_2 measured with continuous-wave ring-down spectroscopy, Phys. Chem. Chem. Phys., 8, 364–368, 2006.

Oyama, H., Morino, I., Nagahama, T., Machida, T., Suto, H., Oguma, H., Ogura, H., Sawa, Y., Matsueda, H., Sugimoto, N., Nakane, H., and Nakagawa, K.: Column-averaged volume mixing ratio of CO_2 measured with ground-based Fourier transform spectrometer at Tsukuba, J. Geophys. Res., 114, D18303, doi:10.1029/2008JD011465, 2009.

Sakamoto, A. and Nishii, J.: Fiber Fabry-Perot interferometer with precision glass-ceramic jacketing, IEEE Photons Tech. Lett., 17, 1462–1464, 2005.

Washenfelder, R. A,, Toon, G. C., Blavier. J. -F., Yang. Z., Allen, N. T., Wennberg, P. O., Vay, S. A., Matross, D. M., and Daube, B. C.: Carbon dioxide column abundances at the Wisconsin Tall Tower site, J. Geophys. Res., 111, D22305, doi:10.1029/2006JD007154, 2006.

Wilson, E. L., Georgieva, E. M., and Heaps, W. S.: Development of a Fabry-Perot interferometer for ultra-precise measurements of column CO_2, Meas. Sci. Technol., 18, 1495–1502, 2007.

WMO: WMO Greenhouse Gases Bulletin, The state of greenhouse gases in the atmosphere using global observations though 2008, World Metrological Organization, 2008.

Yokota, T., Yoshida, Y., Eguchi, N., Ota, Y., Tanaka, T., Watanabe, H., and Maksyutov, S.: Global concentrations of CO_2 and CH_4 retrieved from GOSAT: First preliminary results, http://www.jstage.jst.go.jp/browse/sola/5/0/_contents, Scientific Online Letters on the Atmosphere, 5, 160–163, doi:10.2151, 2009.

Table 1. Column densities and column average concentrations of CO_2 at the Moshiri observatory measured by different instruments.

Method	Column Density (10^{21} molecules/cm^2)	Concentration[a] (ppm)	Time of Measurement[b]	Number of Measurements
OSA[c]	7.890±0.028	377.09±1.35	09:40~16:11	70
FTS[d]	7.800±0.081	376.60±3.93	10:19~15:50	84
Balloon	7.934±0.108	378.02±5.16	13:30~14:26	1
FTS-GFIT[e]	ND[f]	377.05±2.47	09:50~16:01	275
Aircraft[g]	ND	376.56±0.02	12:37~13:57	8
GOSAT[h]	7.778±0.034	367.73±1.59	12:48; 6 Aug	1
	7.887±0.030	368.75±1.41	12:47; 2 Sep	1

[a] Column average volume mixing ratio.
[b] 26 August 2009 except GOSAT.
[c] Optical spectrum analyzer, Yokogawa AQ6370B-Custom.
[d] Fourier transform spectrometer, Bruker 120HR. Retrieved by the algorism in the present work (see the Appendix).
[e] Retrieved by NIES using GFIT.
[f] Not determined.
[g] Flask sampling and analyzed by NIES.
[h] Measured over Nayoro City in Hokkaido Japan located 20 km east to the Moshiri observatory.

AMTD
3, 1615–1644, 2010

Table 2. Column densities and column average concentrations of CH_4 at the Moshiri observatory.

Method	Column Density 10^{19} molecules/cm^2)	Concentration[a] (ppm)	Time of Measurement[b]	Number of Measurements
OSA[c]	3.76±0.06	1.796±0.028	09:40~16:11	48
FTS-GFIT[d]	ND[e]	1.725±0.016	09:50~16:01	275
Aircraft[g]	ND	1.841±0.012	12:37~13:57	8
GOSAT[h]	3.64±0.01	1.721±0.004	12:48; 6 Aug	1
	3.69±0.01	1.729±0.005	12:47; 2 Sep	1

[a] Column average volume mixing ratio.
[b] 26 August 2009 except GOSAT.
[c] Optical spectrum analyzer, Yokogawa AQ6370B-Custom.
[d] Retrieved by NIES using GFIT.
[e] Not determined.
[g] Flask sampling and analyzed by NIES.
[h] Measured over Nayoro City in Hokkaido Japan located 20 km east to the Moshiri observatory.

AMTD
3, 1615–1644, 2010

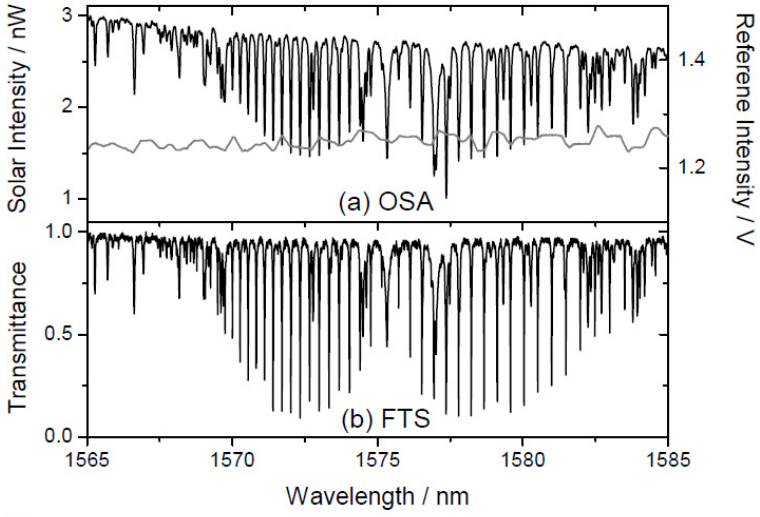

Fig. 1. CO_2 photoabsorption spectra measured by OSA and FTS on 26 August 2009 at Moshiri in Hokkaido, Japan.

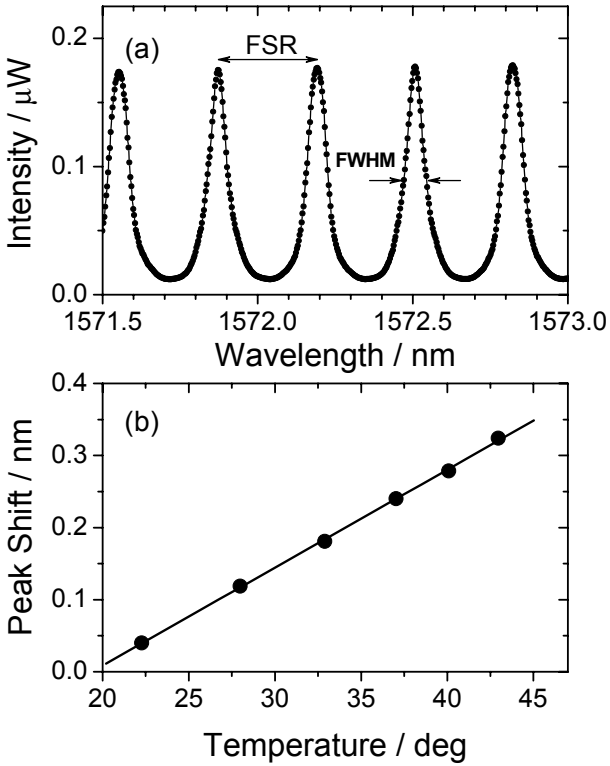

Fig. 2. **(a)** Free spectral range (FSR=0.317±0.002 nm) and full-width at half maximum (FWHM=0.072±0.002 nm) of FFPI; **(b)** Spectral shift of the transmission wavelength by temperature. Temperature coefficient=13.58±0.16 pm/deg.

AMTD
3, 1615–1644, 2010

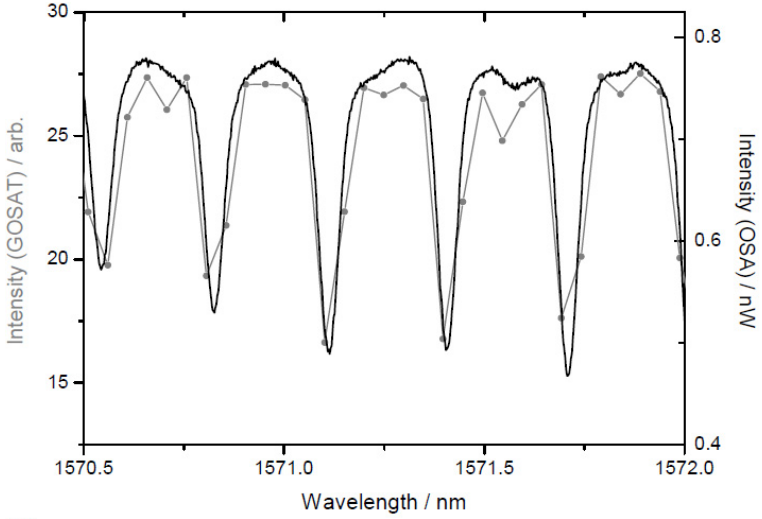

Fig. 3. Parts of CO_2 photoabsorption spectra measured by OSA and FTS onboard GOSAT. OSA: black curve; GOSAT: gray line with dots.

AMTD
3, 1615–1644, 2010

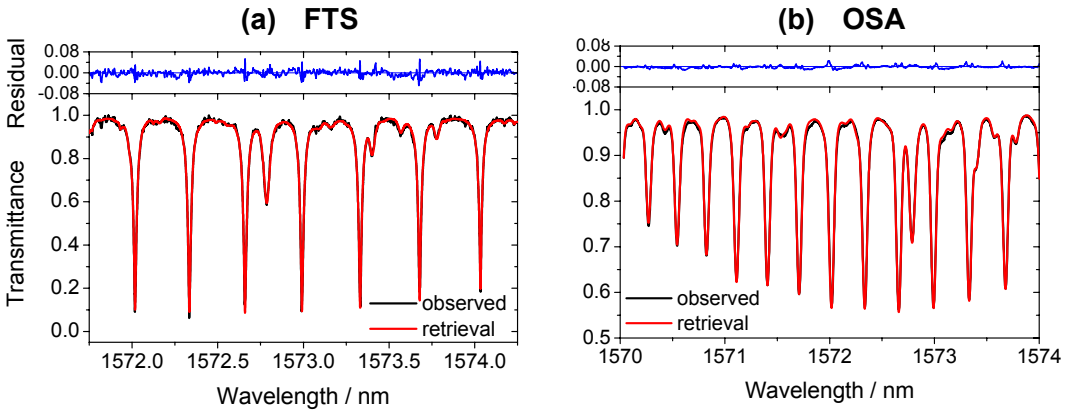

Fig. 4. Enlarged spectra shown in Fig. 1 for the OSA and the FTS after retrievals. Black curves denote the observed spectra and red ones for the retrievals.

AMTD
3, 1615–1644, 2010

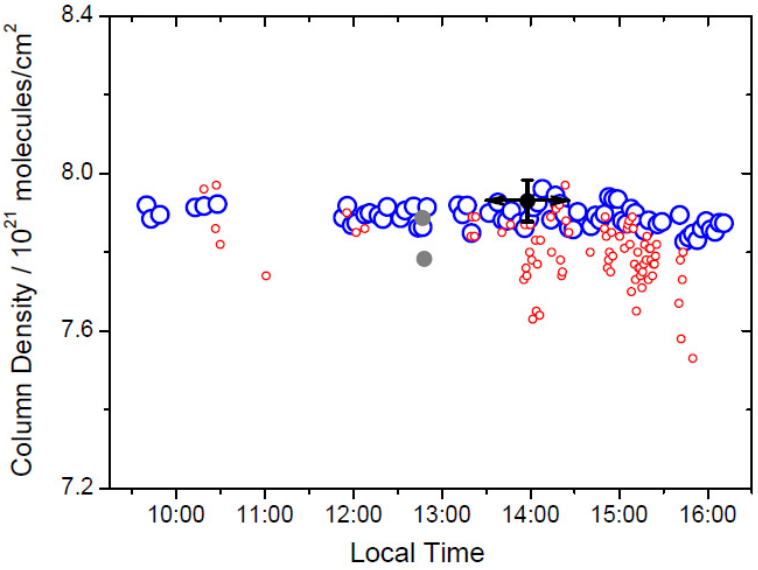

Fig. 5. CO_2 column density profile measured by OSA, FTS, balloon and GOSAT. OSA: large open circles; FTS: small open circles; Balloon: arrows; GOSAT: gray solid circles.

AMTD
3, 1615–1644, 2010

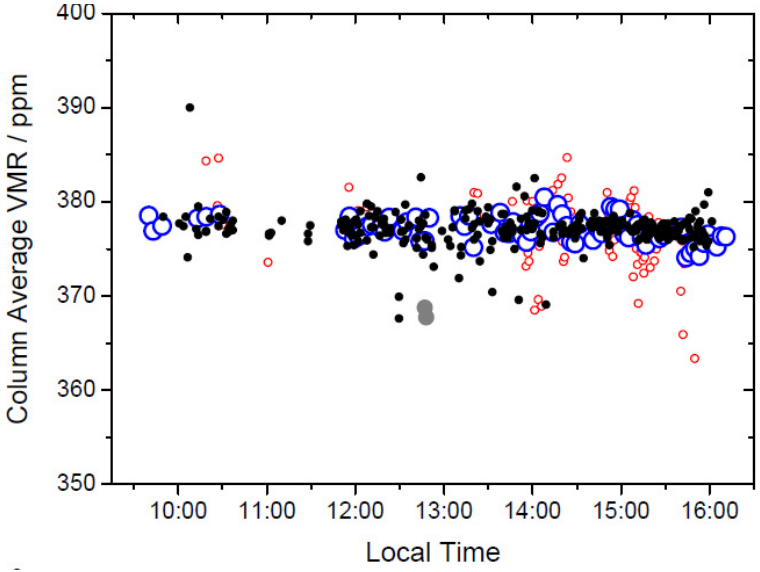

Fig. 6. Column average concentration profile of CO_2. OSA: large open circles; FTS: small open circles; FTS-GFIT: small solid circles; GOSAT: gray solid circles.

AMTD
3, 1615–1644, 2010

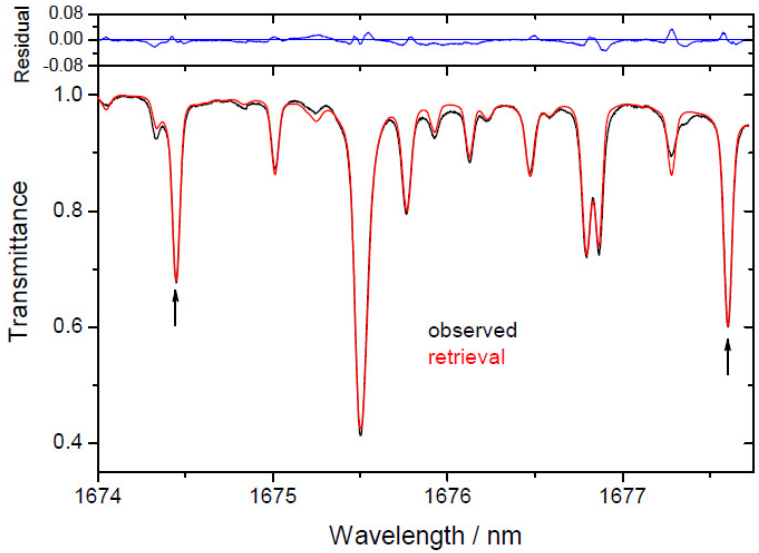

Fig. 7. CH_4 photoabsorption spectrum for OSA retrieval. Black curve denotes the observed spectrum and red one for the retrieval. Arrows are the photoabsorption lines of CH_4.

AMTD
3, 1615–1644, 2010

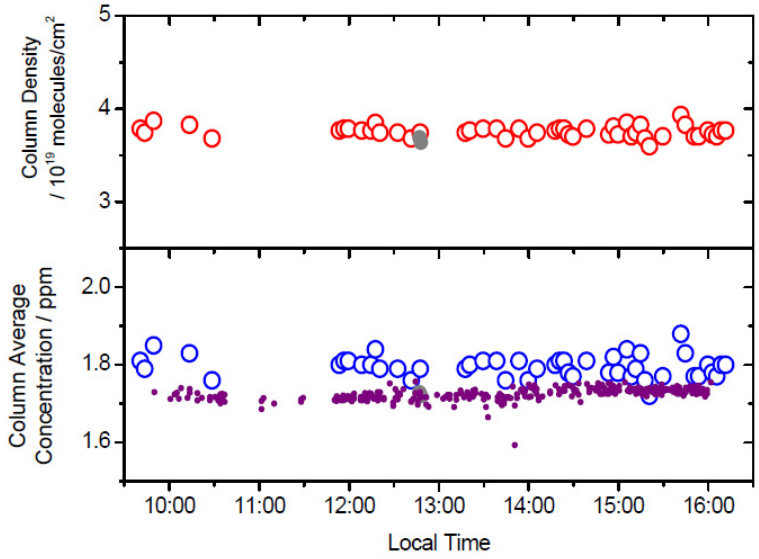

Fig. 8. Column density and column average concentration profiles. OSA: large open circles; FTS-GFIT: small solid circles; GOSAT: gray solid circles.

AMTD
3, 1615–1644, 2010

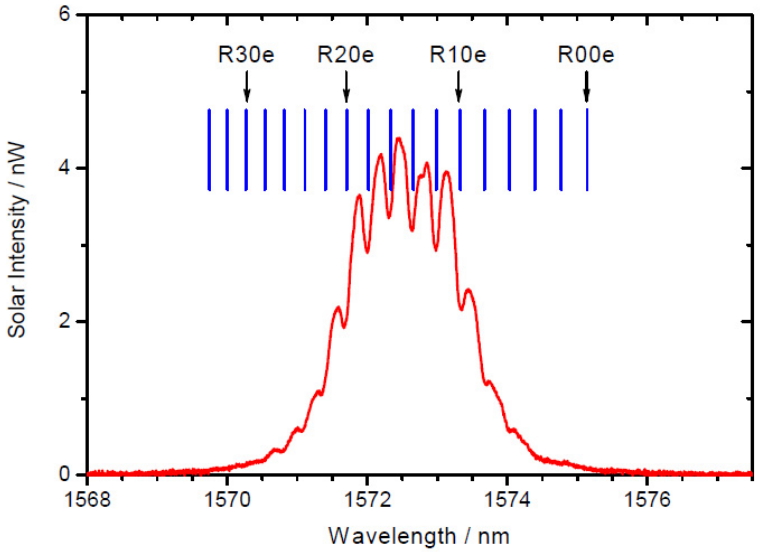

Fig. 9. Spectral profile of the sunlight through a narrow bandpass filter. Assignments for the R-branch in the CO_2(30 012←00 001) transition are shown.

AMTD
3, 1615–1644, 2010

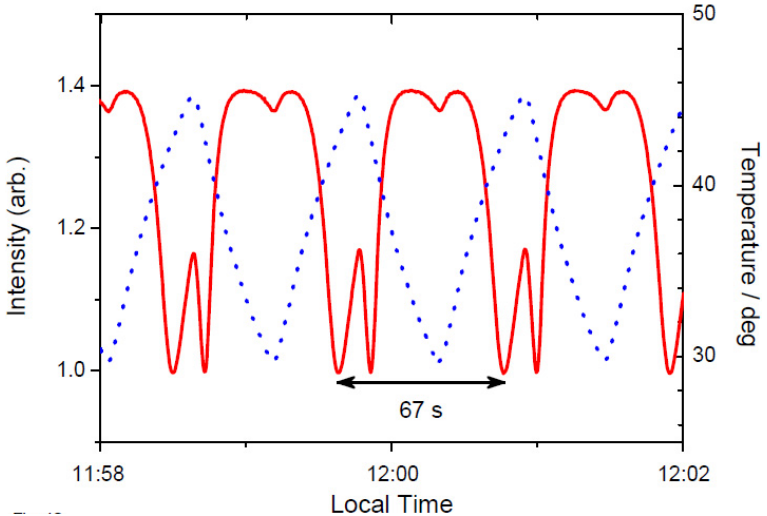

Fig. 10. Signal intensity of the CO_2 photoabsorption (solid curve) measured by modulating the FFPI temperature in a 67 s cycle (dotted curve). The highest value gives the I_0 and the lowest one corresponds to the I value in Eq. (1). Small dip at the top and hump at the bottom result from overshooting the temperature.

AMTD
3, 1615–1644, 2010

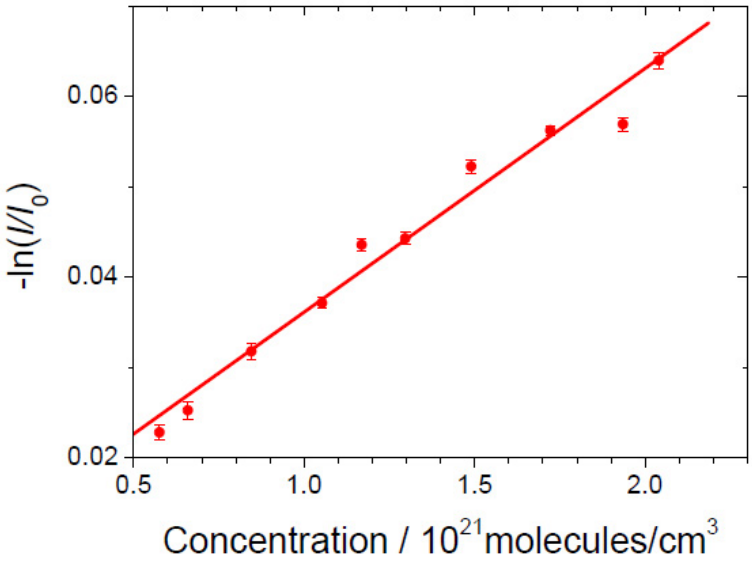

Fig. 11. Absorbance of CO_2 for effective total photoabsorption cross section determination measured in the laboratory with neat CO_2 at room temperature.

AMTD

3, 1615–1644, 2010

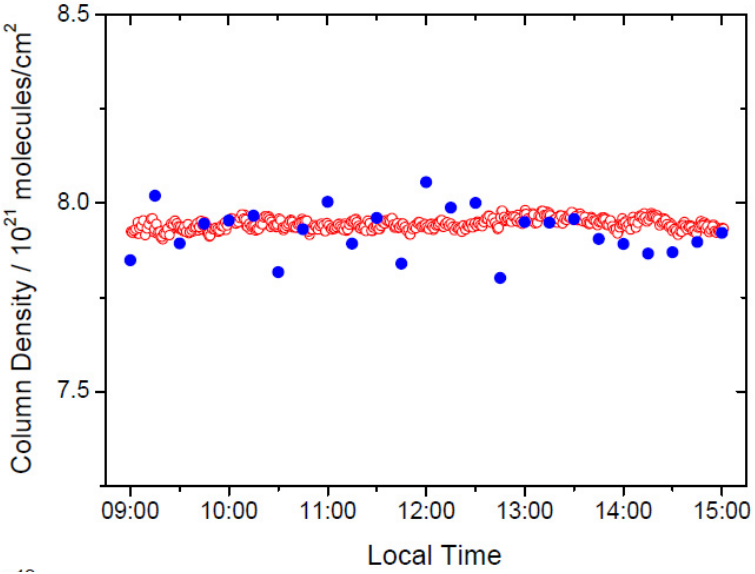

Fig. 12. CO_2 column density measured by FFPI on 31 October 2009 at the Katsura Campus of Kyoto University, Kyoto Japan. Open circles are the CO_2 column densities after normalization and the solid circles are those measured by OSA at the same time.

AMTD
3, 1615–1644, 2010